



HAL
open science

A VLC-based Footprinting Localization Algorithm for Internet of Underwater Things in 6G networks

Anna Maria Vegni, Marwan Hammouda, Valeria Loscri

► **To cite this version:**

Anna Maria Vegni, Marwan Hammouda, Valeria Loscri. A VLC-based Footprinting Localization Algorithm for Internet of Underwater Things in 6G networks. IEEE 5th International Workshop on Optical Wireless Communications (IWOW), Sep 2021, Berlin, Germany. hal-03282673

HAL Id: hal-03282673

<https://hal.science/hal-03282673>

Submitted on 9 Jul 2021

HAL is a multi-disciplinary open access archive for the deposit and dissemination of scientific research documents, whether they are published or not. The documents may come from teaching and research institutions in France or abroad, or from public or private research centers.

L'archive ouverte pluridisciplinaire **HAL**, est destinée au dépôt et à la diffusion de documents scientifiques de niveau recherche, publiés ou non, émanant des établissements d'enseignement et de recherche français ou étrangers, des laboratoires publics ou privés.

A VLC-based Footprinting Localization Algorithm for Internet of Underwater Things in 6G networks

Anna Maria Vegni
Dept. of Engineering
Roma Tre University
annamaria.vegni@uniroma3.it

Marwan Hammouda
marwan.hammouda@gmail.com

Valeria Loscri
FUN Research-lab
INRIA Lille-Nord Europe
valeria.loscri@inria.fr

Abstract—In the upcoming advent of 6G networks, underwater communications are expected to play a relevant role in the context of overlapping hybrid wireless networks, following a multi-layer architecture *i.e.*, aerial-ground-underwater. The concept of Internet of Underwater Things defines different communication and networking technologies, as well as positioning and tracking services, suitable for harsh underwater scenarios.

In this paper, we present a footprinting localization algorithm based on optical wireless signals in the visible range. The proposed technique is based on a hybrid Radio Frequency (RF) and Visible Light Communication (VLC) network architecture, where a central RF sensor node holds an environment channel gain map *i.e.*, database, that is exploited for localization estimation computation. A recursive localization algorithm allows to estimate user positions with centimeter-based accuracy, in case of different turbidity scenarios.

Index Terms—Optical wireless communications, underwater communications, localization, visible light.

I. INTRODUCTION

In future 6G networks, hybrid wireless networks are expected to coexist according to a multi-layer structure that consists of overlapping aerial, ground and underwater networks [1]. In the latter environment, it is recently emerging a new communication paradigm developed for connecting underwater things *i.e.*, the Internet of Underwater Things (IoUT) [2]. IoUT technology consists of intelligent devices, such as boats and ships, as well as submarines and other underwater nodes, connected to each other for data communication and sensing, positioning and navigation. Among the main applications, IoUT is envisioned for underwater exploration and monitoring, disaster prediction and prevention.

Due to the particular harsh underwater environment where well-known Global Positioning System (GPS) technology cannot penetrate, positioning and tracking are two challenging tasks. Other wireless technologies are then adopted for localization purpose, including acousting, electromagnetic and Optical Wireless Communications (OWC). Current systems for underwater communication are mainly based on acoustic waves, due to the long distances easily reachable with stable connectivity. However, acoustic links suffer of low data rates over relatively long distances, thus strongly limiting data transmission and inferring longer delays. On the other side, OWC technology –in the visible range– promises higher data rates, low interference, and smaller latency, but with a limited short

communication range. Underwater VLC (UVLC) systems are of particular interest for system engineering specially in the range of green light (*i.e.*, [495, 570] nm) because of a low attenuation window within this band. As a result, UVLC allow to reach high data rates for short Line-of-Sight (LoS) links, based on the visibility between transmitter and receiver affected by the turbidity of the water.

The investigation of UVLC systems has been recently addressed in the research community [3], [4]. However, to the best of authors' knowledge, poor contributions have dealt with underwater localization techniques. Traditionally, Visible Light Positioning (VLP) systems have been largely applied in indoor scenarios [5], where it results easier to install LED devices and noise can be strongly limited. VLP techniques use trilateration [6], angle-of-arrival and time-of-arrival algorithms. Of course, in case of mobility, the LoS constraint is not guaranteed and localization becomes more challenging. As an instance, in [7] a drone tracking VLC approach has been investigated in an industrial environment. On the other side, in harsh environments like the underwater one, localization techniques need to be deployed with particular care. Indeed, the underwater VLP system should take into account the noise due to wave motion, sunlight rays and moving obstacles such as fishes and other water beings that may cause blockage. Furthermore, Light Emitting Diode (LED) and PhotoDetector (PD) devices should be battery-powered, not necessarily relying on an existing infrastructure as occurring in indoor cable scenarios. A similar consideration may apply to any RF device used for uplink communications in VLP systems. Finally, in underwater scenarios the localization task is not limited to the (x, y) plane, but extends to a $V = (x \times y \times z)$ volume, thus representing a more challenging technique. As a result, an efficient underwater VLP system should consider all these constraints. In [8] a hybrid communication underwater system is developed, that combines magnetic communication and VLC links. The formers work independently of LoS requirements and turbidity, but enable lower data rates than VLC.

In this paper, we present a footprinting localization algorithm for IoUT scenarios, based on a hybrid network architecture comprised of both RF and VLC technology. Specifically, we design a VLP system comprised of a set of LED transmitters laying on the seabed, covering a given monitoring space

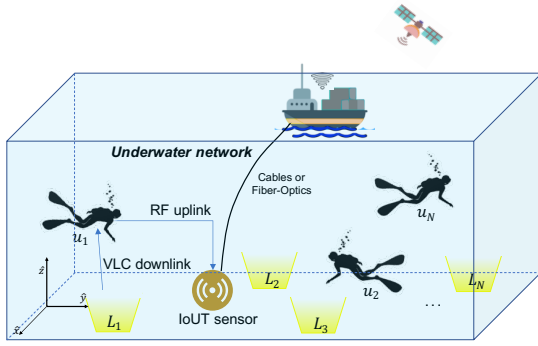


Fig. 1. Schematic of a reference underwater network, comprised of LED transmitters and a centralized RF IoT sensor. Wearable battery-powered photodetectors are assumed to be placed on diver's wetsuit.

by providing a given illumination level. A centralized architecture comprised of a RF device is exploited for localization computational tasks. The proposed VLP technique is based on a footprinting approach, where the channel impulse response coefficients are initially collected in a database, stored in the RF local cache. A similar approach has been previously investigated in indoor environments [6], but limited to 2D position estimations.

This paper is organized as follows. Section II presents the reference system model for underwater VLP, while in Section III the proposed underwater localization algorithm is described. The effectiveness of this approach is addressed in Section IV, through simulation results expressed in terms of estimation error. We observe a localization technique able to achieve high accuracy of the order of few centimeters, while guaranteeing easiness of device deployment and installation. Finally, conclusions are drawn at the end of the paper.

II. SYSTEM MODEL

Let us consider an UVLC network scenario, comprised of a set of LED transmitters $\mathcal{L} = \{L_1, L_2, \dots, L_N\}$ with $L_N \geq 4$, deployed in a given 3D space \mathcal{S} [m³], as depicted in Fig. 1. Notice that in order to omit noise and interference due to sunlight, as well as to reduce the wave movement affecting the stability of LEDs, we assume that the i -th transmitter is posed on the seabed in a fixed known position *i.e.*, $P_i = (x_i, y_i, 0)$, with $i = [1, 2, \dots, N]$. Several users (*e.g.*, divers) are moving in the monitoring space \mathcal{S} , each of them having a wearable photodetector placed on the wetsuit. Specifically, we consider $\mathcal{U} = \{u_1, u_2, \dots, u_M\}$ with $u_M \neq 0$ as the set of PDs in the given area.

We assume that the LED transmitters illuminate the whole space \mathcal{S} so that in each position it is guaranteed a minimum illumination level. As depicted in Fig. 1, the underwater network is comprised not only of LEDs but also of a RF IoT sensor, with computational skills. The RF IoT central node is accordingly deployed with the aim of performing simple computational tasks necessary for the localization algorithm; a simple comparing operation is the only needed operation, which then simplifies the hardware requirements. The IoT

sensor can collect and process the electrical signals at the output of the PDs, in order to estimate the user position according to the proposed localization algorithm. The position estimation data are then transmitted to a control node (*e.g.*, a boat in Fig. 1) for monitoring and tracking tasks.

Notice that the PDs are assumed to be battery-powered, lasting for a given time interval enough for diving tasks. As an example, in 2013 it was launched a new 2-channel diving device for communication at maximum distance of 30 m inside water at depth of 30 m. The device is battery-powered, lasting for up to 240 minutes of communication.

By assuming a LoS link between the i -th LED and the j -th PD, the output signal at the j -th PD is an electrical current $Y(t)$ that can be expressed as

$$Y(t) = rX(t) * h_w(t) + N(t), \quad (1)$$

where $X(t)$ is the transmitted optical intensity waveform of T time duration, r [A/W] is the responsivity of the j -th PD, $h_w(t)$ is the channel impulse response in underwater scenario and $N(t)$ is the shot noise due to ambient light. For sufficiently low rate, $h_w(t)$ can be approximated to the DC gain of an ideal channel *i.e.*, $H_{w,0}$. Also, from [9], we can approximate the channel impulse response in underwater environment according to Beer-Lambert law as follows:

$$H_{w,0} = e^{(-c(\lambda)d_{ij})} \cdot \frac{A_r(m+1)}{2\pi d_{ij}^2} \cos^m(\phi) T_s(\psi) g_j(\psi) \cos(\psi) \text{rect}\left(\frac{\psi}{\psi_c}\right), \quad (2)$$

where A_r [cm⁻²] is the active PD area, ϕ is the angle of irradiance, ψ is the angle of incidence w.r.t. the receiver axis, $T_s(\psi)$ and $g(\psi)$ are the gains of the optical filter and of the optical non-imaging concentrator, respectively. We assume $T_s(\psi) = 1$ and $g_j(\psi) = n^2/\sin^2(\psi)$, with ψ_c as the Field of View (FOV) of the j -th PD *i.e.*, the maximum angle at which the light emitted by the i -th LED is detected by the j -th PD, and n as the refraction index. In addition, $m = -\ln(2)/\ln(\cos(\psi_{1/2}))$ is the Lambertian order, where $\psi_{1/2}$ is the LED half intensity viewing angle, and $\text{rect}(x) = 1$ if $|x| \leq 1$ and $\text{rect}(x) = 0$ otherwise.

In Eq. (2), the exponent $c(\lambda)$ represents the extinction coefficient, which takes into account both the absorption coefficient *i.e.*, $a(\lambda)$, and the scattering coefficient *i.e.*, $b(\lambda)$, for a given wavelength λ [nm] in a specified water type:

$$c(\lambda) = a(\lambda) + b(\lambda). \quad (3)$$

Specifically, we consider different water types, such as pure sea, clear ocean, coastal water and harbor water, whose corresponding extinction coefficients are respectively [0.056, 0.150, 0.305, 2.170] m⁻¹. Notice that higher (lower) values of the extinction coefficient correspond to turbid (non-turbid) water. Then, pure sea and clear ocean are considered as non-turbid water, whereas the coastal and harbor water can be considered as turbid water [10]. It is expected that, due to water conditions affecting visibility, in turbid water the position estimation error will be higher than the case of non-turbid water.

III. LOCALIZATION ALGORITHM IN UNDERWATER NETWORK

In this section, we describe the localization process adapted in this paper for the underwater scenario. This process is mainly composed of three major phases. Initially, the channel responses between each of the (four) LEDs and each location within the entire space of interest are measured and stored in a map, also referred as database. This database can be generated off-line and it might be updated periodically over certain time intervals. As already highlighted, in this paper we assume a centralized localization process in which an RF-based simple IoT sensor is responsible for the entire localization process. This indeed has a significant practical advantage, as the database should be known only to this IoT device and not to any of the edge devices, *i.e.*, LEDs or users.

It should be noted, that unlike the widely-investigated indoor environments in which the user moves within a 2-dimensional (2D) space (normally defined as the (x, y) space in the Cartesian coordinates), a given user in the underwater environment can move within a 3D space, *i.e.*, along the three x -, y -, and z -coordinates. Thus, a 3D database would be generated and stored in the IoT sensor. To facilitate building this database, we consider a spatial sampling concept in which the entire (3D) space is designed as a 3D grid and each point in this grid is considered as a possible user location. Specifically, the whole 3D space is modeled as $\mathcal{S} = N_x \times N_y \times N_z$ samples, where

$$N_x = l_x \cdot \Delta x, \quad N_y = l_y \cdot \Delta y, \quad \text{and} \quad N_z = l_z \cdot \Delta z, \quad (4)$$

where $l_{x,y,z}$ [m] are the space dimensions along $\{x, y, z\}$ directions and $\Delta\{x, y, z\}$ (with $0 < \Delta\{x, y, z\} \leq 1$) are the sampling rates along the corresponding orthogonal directions. Notice that lower is $\Delta\{x, y, z\}$, higher will be the accuracy of the localization algorithm. Indeed, reducing the gap between adjacent points in this grid will result in a higher (smaller) localization accuracy (error). However, this would require a larger memory to store this map, which can be seen as a hardware limitation as simple IoT devices are expected to have a very limited memory. As an example, let us consider a $10 \times 10 \times 10 \text{ m}^3$ space with a grid spacing of 1 m along each direction. Thus, we have a total of 4000 values for all grid points and from the four APs. If each of these points will be stored as a 4-Byte float number, then a memory of 16 KByte will be needed. It follows that an accuracy-space trade-off is expected and it should be carefully handled.

Now having the database stored at the IoT device, a localization algorithm can be implemented in the second phase using that database. We consider a simple, still efficient, localization algorithm in which we measure the channel responses between the four LEDs and the user (unknown) location to be estimated, and compare these values with those stored at the database. We then use the clear mapping between channel gains and locations in the database to estimate the user location. The main challenge of the proposed localization technique is to reduce the number of locations that can be

considered as potential user locations. To handle this issue, we consider a recursive algorithm in which we aim at minimizing the set of possible user locations at each localization algorithm step.

Before proceeding, we should stress that the recursive algorithm detailed below is based on the assumption that the channel gain contribution of each LED at the (unknown) user location are known beforehand. This assumption is indeed required by other algorithms based on the received signal strength indicator (RSSI). However, the localization algorithm described here, which is based on a stored database, has a fundamental advantage that no requirements are needed on the number of LEDs covering the user location to guarantee good localization accuracy. For instance, the triangulation algorithm based on the RSSI requires a minimum of three APs to obtain reasonable results. Thus, the algorithm in this paper is expected to obtain reasonable results with much less LEDs covering the entire space¹.

Having this important remark in mind, we now describe the proposed localization algorithm. Let us assume four LED transmitters are deployed in the underwater scenario as depicted in Fig. 1. The i -th user (*i.e.*, u_i) is being located at an unknown location $P_i = (x_i, y_i, z_i)$, then the target is to get the location estimate $\hat{P} = (\hat{x}_i, \hat{y}_i, \hat{z}_i)$. To this end, the proposed localization algorithm goes through the following three steps *i.e.*, (i) database construction, (ii) likely position detection, and (iii) position estimation.

Step I. Database construction: This first step corresponds to the construction of an underwater scenario channel gain database, namely \mathcal{D} , which is then stored in the RF sensor node. Let \mathcal{D} carries all the channel responses between all LED transmitters and all the possible user locations within the underwater environment as defined as 3D space \mathcal{S} *i.e.*,

$$\mathcal{D} = \left[\mathbf{h}_1^{(\mathcal{S})}, \mathbf{h}_2^{(\mathcal{S})}, \mathbf{h}_3^{(\mathcal{S})}, \mathbf{h}_4^{(\mathcal{S})} \right], \quad (5)$$

where the j -th \mathbf{h} , with $j = [1, 2, 3, 4]$, is a 3-D matrix of dimensions $N_x \times N_y \times N_z$, whose elements are the channel impulse responses from the j -th LED. The database \mathcal{D} is timely updated in order to compute the position estimation as much correct as real. Indeed, if the database collects channel impulse responses from a water environment type that does not reflect the real scenario, then the position estimation can be badly affected. Finally, the database is stored in the RF sensor local cache.

Step II. Likely position detection: For a given unknown position (*i.e.*, P_i) of the i -th user within the monitoring space \mathcal{S} , we denote the vector carrying the channel impulse responses between all (four) LEDs and the position P_i as $\mathbf{h}^{(P_i)}$, *i.e.*,

$$\mathbf{h}^{(P_i)} = \left[h_1^{(P_i)}, h_2^{(P_i)}, h_3^{(P_i)}, h_4^{(P_i)} \right]. \quad (6)$$

¹Considering a $10 \times 10 \times 10 \text{ m}^3$ space, our simulations showed a very good positioning accuracy with only more than two LEDs. However, we do not show these results in this paper due to the space limitation.

Notice that the smaller the distance between P_i and a given LED, the larger the corresponding channel gain.

The position estimation algorithm starts by comparing the channel gains at the database to the ones measured along the user path. As a result, the algorithm will form several subsets of the database, collecting the possible user locations, till reaching the position estimation. Let us assume $\mathcal{D}^{(1)} \subset \mathcal{D}$, as the first subset of the possible user locations, obtained by comparing the channel gains at the database, *i.e.*, $h_\ell^{(\mathcal{D})}$ for $\ell = \{1, 2, 3, 4\}$, with the largest measured channel gain, *i.e.*, $h_l^{(P_i)} = \max \mathbf{h}^{(P_i)}$. Specifically, the subset $\mathcal{D}^{(1)}$ contains all the user locations whose channel responses satisfy the following criteria:

$$-\xi_h \leq h_\ell^{(\mathcal{D})} - h_l^{(P_i)} \leq \xi_h, \quad (7)$$

where ξ_h is a predefined deviation factor.

The subset $\mathcal{D}^{(1)}$ will be further updated to reduce the number of possible user locations. In particular, the channel gains at the subset $\mathcal{D}^{(1)}$ will be compared with the second largest channel gain in $\mathbf{h}^{(P_i)}$. As a result, the second subset $\mathcal{D}^{(2)} \subset \mathcal{D}^{(1)}$ will be created, which contains all the user locations whose channel responses match the following limits:

$$-2\xi_h \leq h_\ell^{(\mathcal{D}^{(1)})} - \tilde{h}_l^{(P_i)} \leq 2\xi_h, \quad (8)$$

where $\tilde{h}_l^{(P_i)} = \max \mathbf{h}^{(P_i)}$ is the updated (second) largest channel gain in $\mathbf{h}^{(P_i)}$. To further reduce the set of possible user locations, subset $\mathcal{D}^{(3)} \subset \mathcal{D}^{(2)}$ is created with all the locations of the i -th user whose channel gains satisfy Eq. (8) with now $\tilde{h}_l^{(P_i)}$ being the third largest channel gain in $\mathbf{h}^{(P_i)}$ and $h_\ell^{(\mathcal{D}^{(1)})}$ being replaced with $h_\ell^{(\mathcal{D}^{(2)})}$. Finally in this step, the subset $\mathcal{D}^{(4)} \subset \mathcal{D}^{(3)}$ is created with the i -th user locations whose channel gains satisfy Eq. (8) with $\tilde{h}_l^{(P_i)}$ being the last largest channel gain in $\mathbf{h}^{(P_i)}$ and $h_\ell^{(\mathcal{D}^{(1)})}$ being replaced with $h_\ell^{(\mathcal{D}^{(3)})}$. Notice that, for general scenarios with more than four LEDs, this step will keep running till the smallest element in $\mathbf{h}^{(P_i)}$, which will result in the subset $\mathcal{D}^{(L_N)} \subset \mathcal{D}^{(L_N-1)}$, where L_N is the number of LEDs.

Step III. Position estimation: In this step, the localization algorithm estimates the user location using the finally-reduced subset of possible user locations, *i.e.*, $\mathcal{D}^{(4)}$. In particular, the estimation process depends on the cardinality of $\mathcal{D}^{(4)}$, *i.e.*, $|\mathcal{D}^{(4)}|$, as detailed in the following. In the best-case scenario when the subset $\mathcal{D}^{(4)}$ has only one single possible location P_{Rx_k} , *i.e.*, $\mathcal{D}^{(4)} = \{P_{Rx_k}\}$, then the algorithm simply selects the only position as the estimated user location, *i.e.*,

$$\hat{P}_i = P_{Rx_k}. \quad (9)$$

Notice that the position index k refers to the k -th user position as defined in the (original) stored database, as the corresponding index with respect to the subset $\mathcal{D}^{(4)}$ will always be one for this specific case.

However, if the number of the possible locations in the subset $\mathcal{D}^{(4)}$ is greater than one, *i.e.*, $|\mathcal{D}^{(4)}| > 1$, then the

Algorithm 1 Underwater VLP approach

- 1: **Step I: Database construction** (offline)
 - 2: **Initialization:** \mathcal{L} , l_x , Δx , l_y , Δy , l_z , Δz , and c
 - 3: **for** all positions within the 3D space \mathcal{S} **do**
 - 4: Compute \mathbf{h}_j^S for $j = \{1, 2, 3, 4\}$ \triangleright Channel responses are computed using Eq. (2).
 - 5: **end for**
 - 6: Construct the database as in Eq. (5).
 - 7: **Step II: Likely position detection** (at real time)
 - 8: **Initialization:** \mathcal{D} , P_i , c , L_N , and ξ_h
 - 9: Define the channel response vector $\mathbf{h}^{(P_i)}$ as in Eq. (6)
 - 10: $[\mathbf{h}_{\text{sorted}}^{(P_i)}, \mathcal{I}_{\text{sorted}}] = \text{sort}(\mathbf{h}^{(P_i)})$ \triangleright sorting in an ascending order (max to min). $\mathcal{I}_{\text{sorted}}$: set of sorting indexes.
 - 11: **for** $k = 1 : L_N$ **do**
 - 12: **if** $k = 1$ **then**
 - 13: Set $\alpha_1 = -\xi_h$ and $\alpha_2 = \xi_h$
 - 14: Set $\mathcal{D}^{(0)} = \mathcal{D}$
 - 15: **else**
 - 16: Set $\alpha_1 = -2\xi_h$ and $\alpha_2 = 2\xi_h$
 - 17: **end if**
 - 18: Set $\tilde{h}_l^{(P_i)} = \mathbf{h}^{(P_i)}[k]$ and $j = \mathcal{I}_{\text{sorted}}[k]$ \triangleright here, $\mathbf{x}[k]$: k -th element of vector \mathbf{x}
 - 19: Let \mathcal{I}_k be the set of user indexes that satisfy $\alpha_1 \leq \mathcal{D}^{(k-1)}[L_j] - \tilde{h}_l^{(P_i)} \leq \alpha_2$
 $\triangleright \mathcal{D}^{(k-1)}[L_j]$: channel responses in the database for the j -th LED
 - 20: Set $\mathcal{D}^{(k)} = \mathcal{D}^{(k-1)}[\mathcal{I}_k]$ $\triangleright \mathcal{D}^{(k-1)}[\mathcal{I}_k]$: all channel responses in subset $\mathcal{D}^{(k-1)}$ for users with indexes \mathcal{I}_k
 - 21: **end for**
 - 22: **Step III: Position estimation**
 - 23: **for** $j = 1 : |\mathcal{D}^{(L_N)}|$ **do**
 - 24: Calculate P_j using Eq. (10) $\rightarrow \mathbf{p}[j] = P_j$
 - 25: **end for**
 - 26: Sort \mathbf{p} in an ascending order $\rightarrow \mathbf{p}_{\text{sorted}} = \text{sort}(\mathbf{p})$
 - 27: Let P_{Rx_i}, P_{Rx_j} be the two users whose indexes result in the first two estimates in $\mathbf{p}_{\text{sorted}}$
 - 28: Estimate the user position using Eq. (11)
-

algorithm calculates the estimates \hat{P}_j for $j = 1, \dots, |\mathcal{D}^{(4)}|$ as follows:

$$\hat{P}_j = \sum_{l=1}^4 |h_l^{(P_i)} - h_{\ell,j}^{(\mathcal{D}^{(4)})}|, \quad (10)$$

where $h_l^{(P_i)}$ is the measured channel gain between the l -th LED and the i -th user location, as defined in Eq. (6), and $h_{\ell,j}^{(\mathcal{D}^{(4)})}$ is the stored channel gain between the ℓ -th LED and the j -th user location at the subset $\mathcal{D}^{(4)}$. The algorithm then selects the user locations with the largest two estimates (*i.e.*, P_{Rx_m}, P_{Rx_n}), and the estimated user location will be the corresponding average *i.e.*,

$$\hat{P}_i = \text{avg}\{P_{Rx_m}, P_{Rx_n}\} = \left[\frac{x_{Rx_m} + x_{Rx_n}}{2}, \frac{y_{Rx_m} + y_{Rx_n}}{2}, \frac{z_{Rx_m} + z_{Rx_n}}{2} \right], \quad (11)$$

TABLE I
MAIN PARAMETERS USED IN THE SIMULATIONS

Parameter	Values
LED Power	10 W
Beam angle	50°
Monitoring space \mathcal{S} ($l \times w \times h$)	10 m \times 10 m \times 10 m
FOV	60°
Effective PD area A_e	$1e - 4$ m ²

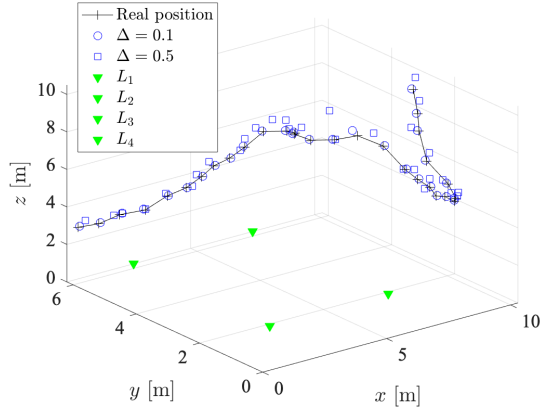


Fig. 2. Estimated and real diver path for different Δ values and in case of pure water *i.e.*, $c = 0.056$ m⁻¹.

where $P_{Rx_m} = [x_{Rx_m}, y_{Rx_m}, z_{Rx_m}]$ and $P_{Rx_n} = [x_{Rx_n}, y_{Rx_n}, z_{Rx_n}]$. Again, the indexes refer to those as defined in the stored database. A detailed pseudocode of the proposed UVLP technique is summarized in Algorithm 1.

The effectiveness of the localization algorithm is then computed through the estimation error of the i -th user position P_i , for different x , y and z directions *i.e.*, $\mathcal{E}_{\{x,y,z\}}^{(P_i)}$ [m], defined respectively as:

$$\mathcal{E}_x^{(P_i)} = \hat{x}_i - x_i, \quad \mathcal{E}_y^{(P_i)} = \hat{y}_i - y_i, \quad \mathcal{E}_z^{(P_i)} = \hat{z}_i - z_i. \quad (12)$$

Based on specific applications, the accuracy of the localization algorithm reflects in the following constraint:

$$\mathcal{E}_{\{x,y,z\}}^{(P_i)} \leq \zeta, \quad (13)$$

where ζ is the localization upper threshold. As an instance, in case of environmental monitoring, we can assume $\zeta = 20$ cm.

Remark 1: In this paper, we ignore the impact of the additive white noise on the measured channel gains, collected in Eq. (6). This is because we mainly target exploring the impact of the underwater environment, basically the water conditions, on the localization accuracy. We recall that this paper, to the best of authors' knowledge, is the first paper in the area of VLP for underwater environments. The impact of the noisy channel gain will be further regarded in an extended study following this paper.

IV. SIMULATED RESULTS

In this section, we aim to assess the effectiveness of the proposed underwater localization algorithm, expressed

in terms of positioning accuracy for different water types. Specifically, we assume a diver (*i.e.*, u_j) is moving in a given underwater network, covering a 3D space of $10 \times 10 \times 10$ m³. According to Fig. 1, four LEDs are placed on the seabed in the following positions *i.e.*, $L_1 = [2.7, 1.9, 0]$, $L_2 = [2.7, 6.2, 0]$, $L_3 = [7.5, 1.9, 0]$, and $L_4 = [7.5, 6.2, 0]$, and the positioning estimation has been computed for $\Delta = [0.1, 0.5]$. Also, two water scenarios *i.e.*, (i) pure sea and (ii) clean ocean, are considered. More details about the simulation setup are collected in Table I.

Fig. 2 depicts the estimated (*blue marks*) and real (*black curve*) path of a diver moving in the considered scenario, assuming a pure water. At a first sight, we can observe the accuracy error in the positioning estimate increases for higher value of Δ , while a reduced error is obtained for lower Δ . However, small estimation errors are due to the low turbidity of the environment. The dependence of the estimation error on the water turbidity can be noticed in Fig. 3 where the estimation error along different directions is computed, by varying the water type. For increasing the extinction coefficient, the error gets worst, reaching a maximum value of ≈ 0.8 [m] in case of harbor water. However, we observe that higher errors are mainly along the x and y -directions, while the estimation error along the z -direction is limited to 0.4 m, as depicted in Fig. 3 (c).

Finally, it is worth to observe that the proposed localization algorithm works efficiently *i.e.*, Eq. (13) holds, when the database is correctly updated to reflect the water type of the monitoring 3D area. However, in case that the database is not correctly updated, the stored channel gains do not correspond to the measured ones, thus causing higher *unacceptable* estimation errors. Let us consider the monitoring space is not homogeneous *i.e.*, the water type is not constant in the space \mathcal{S} . Then, we assume that each LED is immersed in a specific water type, while the stored database has been computed for a unique homogeneous water type. As an instance, due to pollution and water movement, we can assume that LED L_1 and L_4 are immersed in a coastal water (with $c(\lambda) = c_{L_1, L_4} = 0.305$), while LED L_2 and L_3 are in clear (with $c(\lambda) = c_{L_2} = 0.150$) and pure water (with $c(\lambda) = c_{L_3} = 0.056$), respectively. On the other side, we assume that the database has been constructed assuming a clear ocean water type, homogeneous in the whole monitoring space.

In this non-homogenous underwater scenario, the path loss behavior follows the trend depicted in Fig. 4, with higher values close to LED L_1 and L_4 that are immersed in a water type approximated as coastal water, while lower path loss values occur close to LED L_2 and L_3 with extinction coefficients reflecting clear and pure water, respectively. Finally, Fig. 5 shows the estimation error in case of missing match between the channel gains stored in the database and those measured in real time. The missing update of the database reflects in very high estimation errors *i.e.*, $\zeta \gg 0.2$, which are not acceptable for any localization applications.

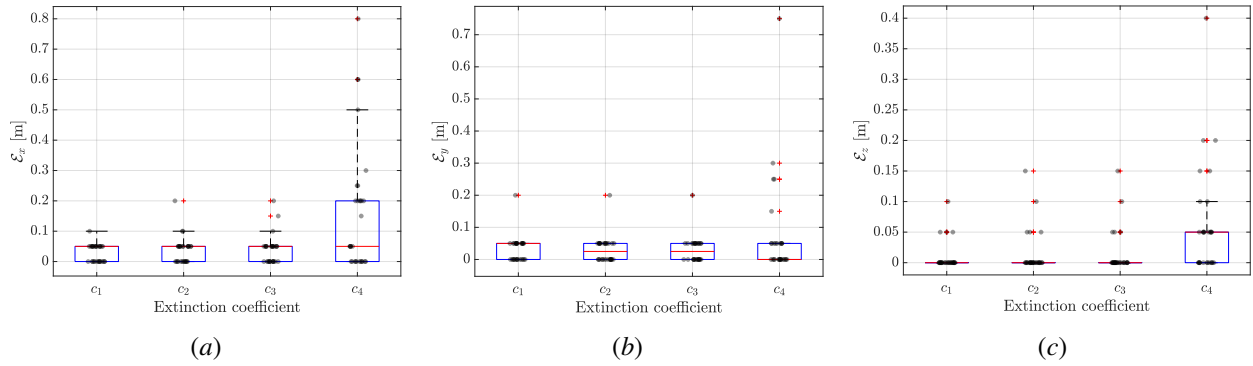


Fig. 3. Estimation error along (a) x , (b) y , and (c) z directions for different water types, expressed in terms of extinction coefficients.

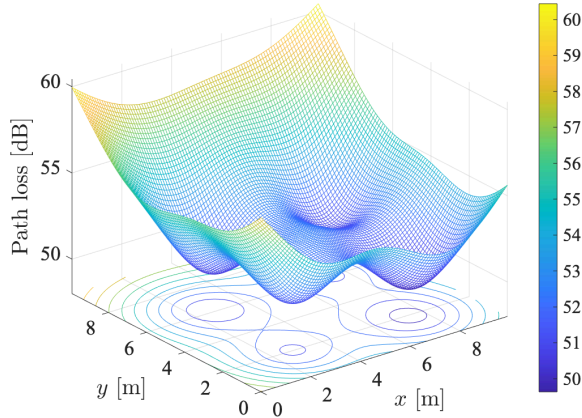


Fig. 4. Path loss [dB] in the hybrid underwater scenario.

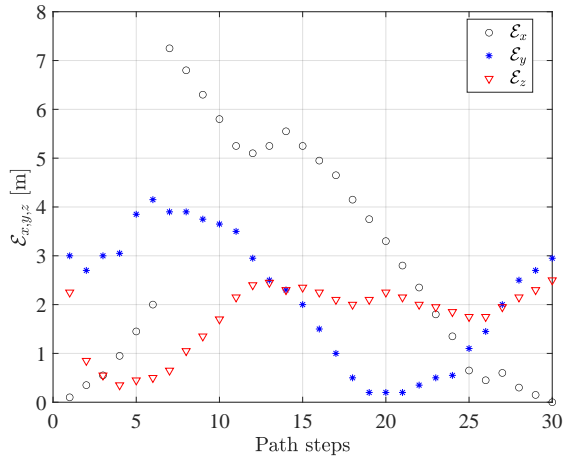


Fig. 5. Estimation error in a hybrid water type scenario, assuming the database does not correctly match the real environment.

V. CONCLUSIONS

A VLC-based footprint localization algorithm working in IoUT framework has been presented in this paper. The proposed approach is based on a recursive method, which compares the channel gains from multiple VLC links, to those

previously stored in a database. Simulation results show the achievable estimation error is limited to few centimeters, with variable errors due to the turbidity of the water. Independently from the localization algorithm, it is important to have a correct database, reflecting the real underwater environment.

VI. ACKNOWLEDGEMENT

This work has been partially supported by a grant from EDESMART project. This article is based upon work from COST Action NEWFOCUS CA19111, supported by COST (European Cooperation in Science and Technology).

REFERENCES

- [1] M. W. Akhtar, S. A. Hassan, R. Ghaffar, H. Jung, S. Garg, and M. S. Hossain, "The shift to 6G communications: Vision and Requirements," *Hum. Cent. Comput. Inf. Sci.*, vol. 10, no. 53, p. 27, 2020.
- [2] M. Jahanbakht, W. Xiang, L. Hanzo, and M. R. Azghadi, "Internet of Underwater Things and Big Marine Data Analytics—A Comprehensive Survey," *IEEE Communications Surveys Tutorials*, pp. 1–1, 2021.
- [3] M. Arfan and C. Lakshminarayana, "Vlc for underwater operations: Li-fi solution for underwater short range communication," in *2018 International Conference on Electrical, Electronics, Communication, Computer, and Optimization Techniques (ICEECCOT)*, 2018, pp. 638–642.
- [4] F. Miramirkhani and M. Uysal, "Visible light communication channel modeling for underwater environments with blocking and shadowing," *IEEE Access*, vol. 6, pp. 1082–1090, 2018.
- [5] J. Luo, L. Fan, and H. Li, "Indoor positioning systems based on visible light communication: State of the art," *IEEE Communications Surveys Tutorials*, vol. 19, no. 4, pp. 2871–2893, 2017.
- [6] A. M. Vegni and M. Biagi, "An indoor localization algorithm in a small-cell led-based lighting system," in *2012 International Conference on Indoor Positioning and Indoor Navigation (IPIN)*, 2012, pp. 1–7.
- [7] Y. Almadani, M. Ijaz, S. Rajbhandari, U. Raza, and B. Adebisi, "Dead-zones limitation in visible light positioning systems for unmanned aerial vehicles," in *2019 Eleventh International Conference on Ubiquitous and Future Networks (ICUFN)*, 2019, pp. 419–421.
- [8] M. Hott, A. Harlakin, and P. A. Hoeher, "Hybrid communication and localization underwater network nodes based on magnetic induction and visible light for auv support," in *2020 International Conference on Information and Communication Technology Convergence (ICTC)*, 2020, pp. 66–68.
- [9] F. Miramirkhani and M. Uysal, "Visible light communication channel modeling for underwater environments with blocking and shadowing," *IEEE Access*, vol. 6, pp. 1082–1090, 2018.
- [10] B. Majleseini, A. Gholami, and Z. Ghassemloooy, "A complete model for underwater optical wireless communications system," in *2018 11th International Symposium on Communication Systems, Networks Digital Signal Processing (CSNDSP)*, 2018, pp. 1–5.